Theoretical study of adsorption of lithium atom on carbon nanotube

AUTHOR(S):

Senami, Masato; Ikeda, Yuji; Fukushima, Akinori; Tachibana, Akitomo

CITATION:

Senami, Masato ...[et al]. Theoretical study of adsorption of lithium atom on carbon nanotube. AIP Advances 2011, 1(4): 042106.

ISSUE DATE:

2011

URL:

http://hdl.handle.net/2433/152431

AIP ADVANCES **1**, 042106 (2011)

Theoretical study of adsorption of lithium atom on carbon nanotube

Masato Senami, Yuji Ikeda, Akinori Fukushima, and Akitomo Tachibana[a]
Department of Micro Engineering, Kyoto University, Kyoto 606-8501, Japan

(Received 26 May 2011; accepted 8 September 2011; published online 3 October 2011)

We investigate the adsorption of lithium atoms on the surface of the (12,0) single wall carbon nanotube (SWCNT) by using *ab initio* quantum chemical calculations. The adsorption of one lithium atom on the inside of this SWCNT is favored compared to the outside. We check this feature by charge transfer and regional chemical potential density. The adsorption of multiple lithium atoms on the interior of the SWCNT is studied in terms of adsorption energy and charge transfer. We show that repulsive force between lithium atoms destabilizes a system for the large number of lithium atoms. [doi:10.1063/1.3651182]

I. INTRODUCTION

Carbon nanotubes (CNTs) have been paid much attention since its discovery in 1991,[1] due to their outstanding mechanical and electric properties.[2–5] Very high Young's modulus of CNTs has been predicted by theoretical studies[3] and confirmed in experiments.[4] Electric properties such as conductance are dependent on the radius and chirality of a CNT through the change of band gap.[5,6]

CNTs have been considered as a candidate of anode materials for lithium ion battery. A theoretical study reported that the density of lithium insertion attains LiC_2, since both the interior and exterior of CNTs are suitable for storage.[7] This lithium storage capability is three times higher than that of normal graphite, LiC_6.[8] However, primary experiments reported only a poor increase of the reversible capacity of lithium compared to that of graphite.[9] In addition, a very large amount of irreversible lithium storage was reported. These features suggests that lithium are stored in the inside of CNTs as unavailable form.

It was reported that the reversible capacity is independent of whether the ends of single wall CNTs (SWCNTs) are open, though the amount of lithium storage is increased due to the diffusion into the inside of CNTs.[10] This imply two facts. One is that the direct diffusion through the sidewalls of pristine CNTs is difficult for lithium ions. Second, lithium (not necessarily ions) stored in the interior of CNTs through open ends of CNTs is not suitable for lithium ion battery as reversible resources. In other words, electrolyte molecules and lithium ions solvated with the electrolyte molecules can freely enter into the interior of CNTs, and this inner surface of the CNTs does not provide available site for lithium ion storage, since the inner surface is similar to the basal plane of the graphite in the electrolyte. Recently, some ideas using steric effects are proposed to improve the reversible capacity of lithium ions.[11,12] It was proposed that the electrolyte molecules and the solvated lithium ions are eliminated by screen materials or defects on the end of CNTs and only bare lithium ions are stored in interior of the CNTs after the desolvation of the solvated lithium ions.[12] They argued that the inner surface of CNTs can provide available site for the bare lithium ions. In their results, the density of lithium storage only in the interior of the (12,0) zigzag SWCNT was shown as LiC_6 by *ab intio* quantum chemical calculations.

In this study, we investigate the adsorption of lithium atoms on the surface of the (12,0) SWCNT and the limit of the storage by using *ab initio* quantum chemical calculations. We clarify the difference

[a]Electronic mail: akitomo@scl.kyoto-u.ac.jp

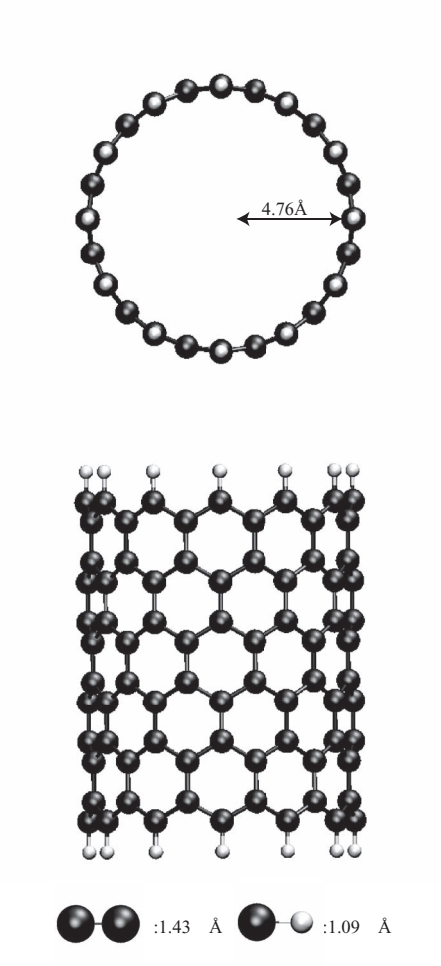

FIG. 1. The (12,0) SWCNT model. Dark (black) circles are carbon atoms, and light (blue) ones are hydrogen atoms.

between the adsorptions on the inside and outside of the SWCNT in viewpoints of charge transfer and regional chemical potential density, which is defined by one of the authors.[13,14] As a result, the advantage of the adsorption on the inside of this SWCNT is shown. We also study the storage density on the interior of the SWCNT in terms of adsorption energy and charge transfer. As a result, we find that the interaction between lithium atoms is a key ingredient for this thin tube. We show that this interaction changes as lithium density increases, in viewpoints of the local charge density

II. COMPUTATIONAL DETAILS

We use the (12,0) zigzag type CNT model. The model is shown in Fig. 1. This model consists of 144 carbon atoms and 24 hydrogen atoms, which are used for the termination of dangling bonds. The structure of this model is determined by the geometrical optimization calculation. The positions of all atoms are relaxed. As a result, the averages of bond lengths are calculated as 1.43 Å for C-C bonds and 1.09 Å for C-H bonds.

In this paper, we study this SWCNT by using *ab initio* quantum chemical calculations. Electronic structure calculations are performed by density functional theory (DFT). In DFT calculations, the Lee-Yang-Parr gradient-corrected functions[15] is selected for the correlation interaction, and it is employed with Becke's hybrid three parameters[16] for generalized-gradient-approximation exchange-correlation functions. These calculations are carried out by GAUSSIAN03 program package.[17] The basis sets are chosen as the 6−31G* basis set for carbon and lithium atoms[18,19] and the 3−21G**

basis set for hydrogen atoms.[19,20] Zigzag SWCNTs with hydrogen termination are known to have spin polarized ground states.[21] Hence, we choose the lowest energy state among all spin multiplicity states in our calculations. Septet state gives the lowest one for the (12,0) CNT without lithium atoms.

We analyze electronic states and properties using quantum energy density, which is proposed by one of the authors.[13,22,23] One of the quantities of the quantum energy density, the electronic kinetic energy density $n_T(\vec{r})$, is defined as,

$$n_T(\vec{r}) = \frac{1}{2}\sum_i \nu_i \left\{ \left[-\frac{\hbar^2}{2m}\Delta\psi_i^*(\vec{r}) \right] \psi_i(\vec{r}) + \psi_i^*(\vec{r}) \left[-\frac{\hbar^2}{2m}\Delta\psi_i(\vec{r}) \right] \right\}, \tag{1}$$

where m is the electron mass, $\psi_i(\vec{r})$ is the ith natural orbital, and ν_i is the occupation number of $\psi_i(\vec{r})$. The integration of kinetic energy density over the whole space is the kinetic energy of a system. In classical mechanics, only positive kinetic energy is allowed, while negative kinetic energy appears in quantum mechanics. This means that electrons can also exist in regions with negative kinetic energy density by quantum effects. The surface of zero kinetic energy density can be interpreted as the boundary of a covalent molecule.

The electronic structure of a system is characterized using electronic stress tensor $\tau^{Skl}(\vec{r})$,

$$\tau^{Skl}(\vec{r}) = \frac{\hbar^2}{4m}\sum_i \nu_i \left[\psi_i^*(\vec{r})\frac{\partial^2\psi_i(\vec{r})}{\partial x^k \partial x^l} - \frac{\partial\psi_i^*(\vec{r})}{\partial x^k}\frac{\partial\psi_i(\vec{r})}{\partial x^l} + \frac{\partial^2\psi_i^*(\vec{r})}{\partial x^k \partial x^l}\psi_i(\vec{r}) - \frac{\partial\psi_i^*(\vec{r})}{\partial x^l}\frac{\partial\psi_i(\vec{r})}{\partial x^k} \right], \tag{2}$$

which describes the internal distortion of electronic density. The three eigenvalues of stress tensor and their eigenvectors determining principal axis can be used for quantitative evaluation of properties of bonding and reactive regions in molecules. The trace over the eigenvalues of stress tensor produces energy density $\epsilon_\tau^S(\vec{r})$ in the non-relativistic limit of the Rigged QED,

$$\epsilon_\tau^S(\vec{r}) = \frac{1}{2}\sum_k \tau^{Skl}(\vec{r}), \tag{3}$$

$$E = \int d^3\vec{r}\,\epsilon_\tau^S(\vec{r}). \tag{4}$$

The ratio of energy density to electronic density gives a linear approximation of the regional electronic chemical potential μ_R,

$$\mu_R = \frac{\delta E_R}{\delta n_R} \approx \frac{\epsilon_\tau^S(\vec{r})}{n_R(\vec{r})}. \tag{5}$$

In this work, the calculations of these quantities of quantum energy density are carried out by using Molecular Regional DFT program package (MRDFT).[24]

III. RESULT AND DISCUSSION

A. The electronic structure of one lithium adsorbed carbon nanotube models

First, we consider the difference between the adsorption of lithium atom on the inside and outside of the (12,0) SWCNT. Optimized structures of the models of (12,0) SWCNTs with one lithium atom are shown in Fig. 2. Panels (a) and (b) show the structures of the CNT with one inside and outside lithium atom, respectively. In geometrical optimization calculations, the positions of all atoms are relaxed. The deformation of the CNT by the attachment of a Li atom is negligibly small. The optimized distances between the Li atom and CNT are 1.87 Å and 1.70 Å for the inside and outside adsorption, respectively.

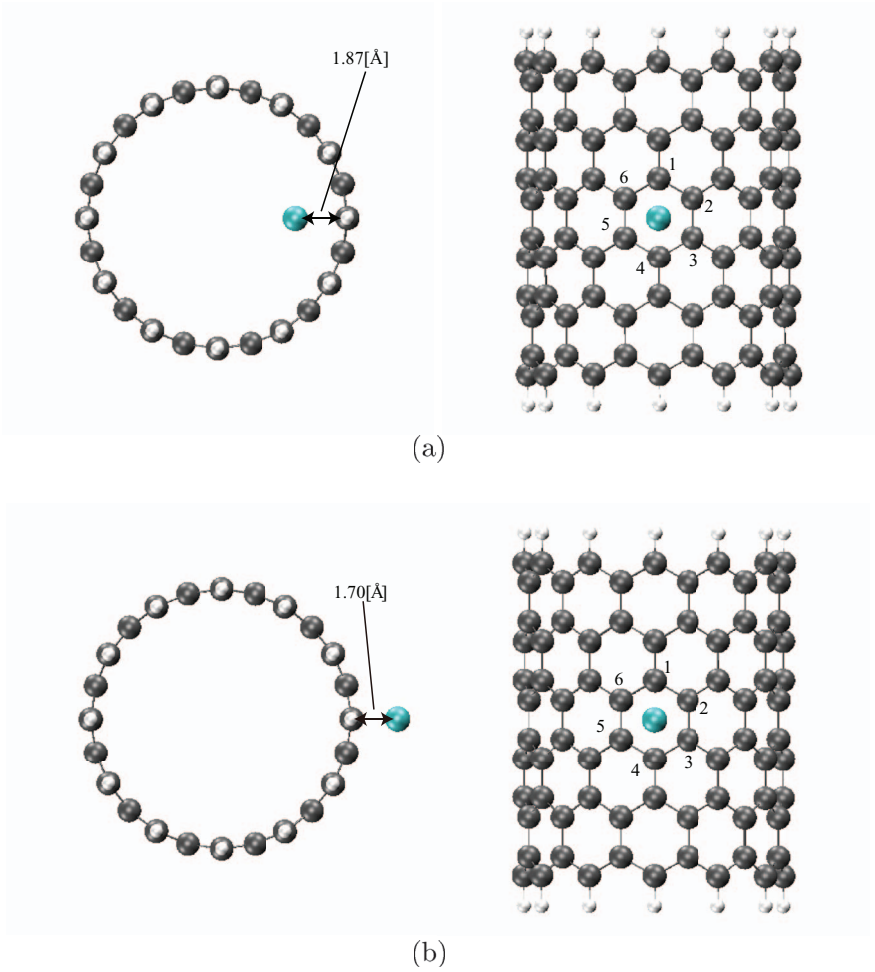

FIG. 2. Optimized structures of the models of (12,0) SWCNTs with one lithium atom. Panels (a) and (b) show the structures of the CNT with one inside and outside lithium atom, respectively.

The lithium adsorption energy in this work is defined as,

$$\Delta E = E_{\mathrm{CNT}+N_{\mathrm{Li}}\times\mathrm{Li}} - E_{\mathrm{CNT}} - N_{\mathrm{Li}} \times E_{\mathrm{Li}}, \tag{6}$$

where E_{Li} is the energy of one lithium atom and N_{Li} is the number of lithium atoms. The adsorption energy of one lithium atom on the inside is -0.98 eV, while that on the outside is -0.86 eV. As a result, the inside of the CNT is more favored for the adsorption of one lithium atom. This is in contrast to some results for the attachment on C_{60}[25], in which exohedral fullerenes are more favored. In the following, we study the reason of the difference of the adsorption energy.

To clarify the interaction between the CNT and the lithium atom, the charge transfer is known to be important.[26,27] Hence, we analyze the NBO charge of the lithium atom. The NBO charge of the lithium atom of the inside of the CNT is calculated as 0.92, while that of the outside is 0.89. This small difference of the charge transfer is attributed to a curvature of the CNT. For the lithium atom on the outside, the nearest carbon atoms are C(1) and C(4), where the position of each carbon atom is shown in Fig. 2 by the number in a parenthesis. On the other hand, the nearest ones are C(2), C(3), C(5), and C(6) for the inside. In addition, the distances from the inside Li atom to carbon atoms in next hexagonal rings are shorter than those from the outside one. Hence, for the inside adsorption, the transfered charge from the Li atom can be distributed for the larger number of carbon atoms.

The distribution of the difference of electron density, i.e., charge transfer, is shown in Fig. 3. The charge transfer is given by the difference of the electron density,

$$\Delta\rho(\vec{r}) = \rho(\vec{r})_{\mathrm{CNT}+N_{\mathrm{Li}}\times\mathrm{Li}} - \rho(\vec{r})_{\mathrm{CNT}} - \rho(\vec{r})_{N_{\mathrm{Li}}\times\mathrm{Li}}, \tag{7}$$

where $\rho(\vec{r})_{\mathrm{X}}$ is the electron density of a system, X. Panels (a) and (b) are the results of the lithium adsorption on the inside of the CNT, while panels (c) and (d) are those for the outside adsorption. Panels (a) and (c) show the plane perpendicular to the axis. Panel (b) (panel (d)) shows the plane including the Li, C(2), and C(3) atoms (Li, C(1), and C(4)), where these carbon atoms are the nearest from the Li atom. The circles in panels (a) and (c) mean the cross section of our CNT model. As seen in Fig. 3, electrons around lithium atoms move to the regions around carbons for both cases. We can see some common properties for both distribution patterns. For example, the electron density decreases behind the lithium atom, and the density increases between Li and C atoms and around C atoms. However, one outstanding feature of the inside adsorption is the larger density increase around carbon atoms in next hexagonal rings as seen in panel (a). This is due to the difference of the distance from the lithium atom as explained above.

In Fig. 4, we show the zero kinetic energy density surface. The definition of the kinetic energy density is given in Eq. (1). Panels (a) and (b) show the results for the same planes in Fig. 3(b) and 3(d), respectively. It has been shown that this quantity classifies whether a bond has covalent property.[13,22,23] The positive kinetic energy region extends between atoms if the bond between the atoms has covalent property. This feature can be seen between carbon atoms in panel (b). For a bond with ionic property, we see two separate positive kinetic energy regions associated with two atoms. As seen in Fig. 4, since the positive kinetic energy regions associated with Li and C atoms are separate for both inside and outside adsorptions, we have confirmed that covalent property is weak and an ionic property is seen for the Li-C bond by our kinetic energy density. Hence, the inside adsorption is favored due to the difference of the charge transfer, which originates in the curved structure of the CNT wall.

Our novel analysis tool, the linear approximation of the regional chemical potential density,[13,14] supports the above conjecture. We show the regional chemical potential density on the zero kinetic energy density surface in Fig. 5. As seen in this figure, the value of the regional chemical potential density of the hexagon on the outer surface is larger than that on the inner surface. As seen in the definition, the regional chemical potential density means the energy per one electron. Our result shows that electrons on the inner surface have lower energy. The region where electrons have lower energy is more favored for the increase of electron density. For the attachment of lithium atoms, the charge is transfered from lithium atoms to the CNT as shown above. Therefore, the interior of isolated SWCNTs is more favorable for the attachment of lithium atoms compared to the exterior of them.

B. The electronic structure of multiple lithium atoms adsorption model

In previous subsection, we have confirmed that the interior of the (12,0) SWCNT is favored for the adsorption of a lithium atom compared to the exterior and shown a reason of this feature. In this subsection, we consider multiple attachment of lithium atoms on the inside of our CNT model.

The structures of the models of (12,0) SWCNTs with lithium atoms are shown in Fig. 6. In panels (a)-(d), two, three, four, and six lithium atoms are attached on the inside of the CNT, respectively. The structure of these models are fully optimized by geometrical optimization calculations. We show also Li-Li and Li-CNT distances in Fig. 6. The deformation of our CNT models are very small. On the other hand, in a result of first principles calculations by other group,[7] the deformation of CNTs by the intercalation of lithium was reported as about 10% in the aspect ratio. In their result, the density of lithium atom are much larger than ours. We consider that their deformation is attributed to the difference of the density. In Fig. 6(b), the Li-Li distance is shorter than that for $Li_2@C_{60}$ whose Li-Li distance is about 3 Å[28]. We consider that this difference of the length is due to a difference of reactivity between our CNT model and C_{60}.

In Fig. 7, the adsorption energy of lithium atoms is shown as a function of the number of lithium atoms, which is defined in Eq. (6). The adsorption energy of four lithium atoms is the largest

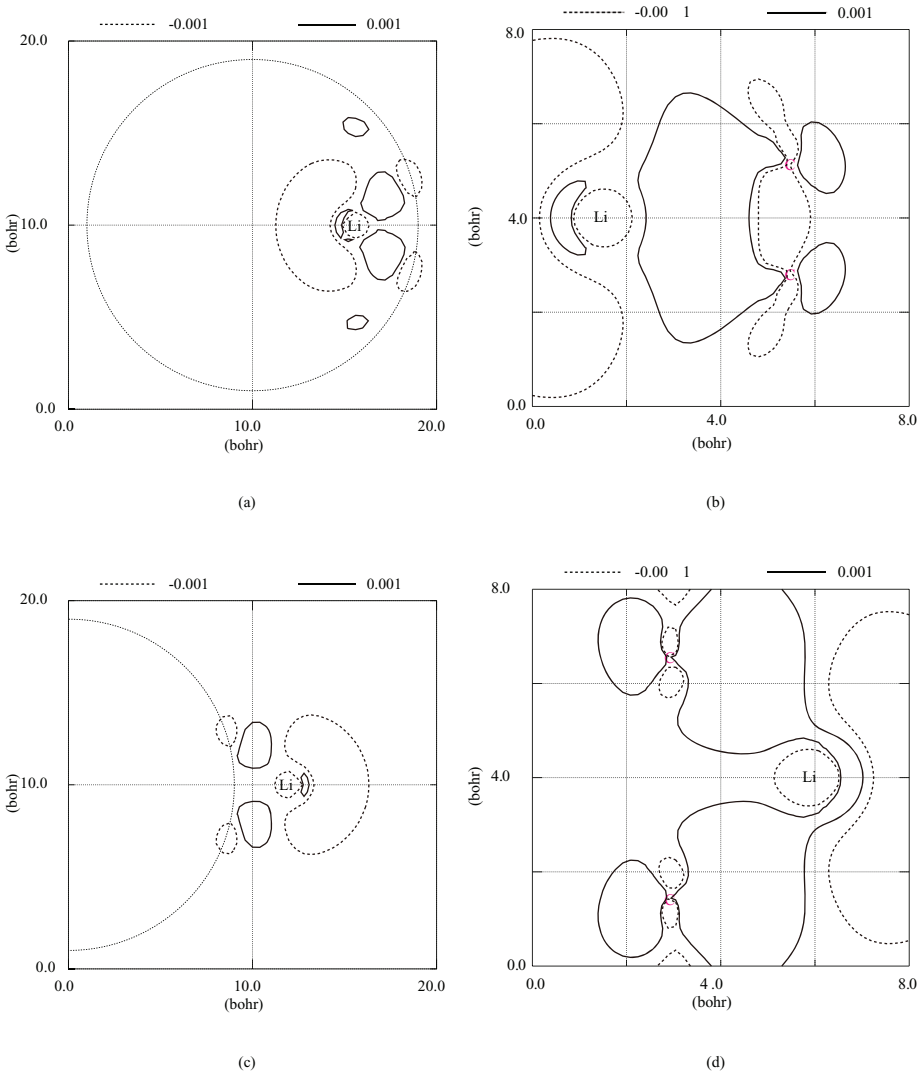

FIG. 3. Distribution of the difference of electron density. Panels (a) and (b) are the results of the lithium adsorption on the inside of the CNT, while panels (c) and (d) are those on the outside. Panels (a) and (c) show the plane perpendicular to the axis. Panel (b) (panel (d)) shows the plane including the Li, C(2), and C(3) atoms (Li, C(1), and C(4)), where a carbon atom specified in a parenthesis corresponds to that shown in Fig. 2. The circles in panels (a) and (c) mean the cross section of our CNT model.

(−1.13 eV) in this result, and the six lithium structure is strongly destabilized from the four lithium structure. This feature is explained from the viewpoint of the Li-Li distance. As seen from Fig. 6, the Li-Li distance becomes short as the number of lithium atoms increases. Particularly, for the insertion of six lithium atoms, Li-Li distances are about 2.9 Å, which is shorter than that of the bulk lithium structure (3.48 Å). Hence, a repulsive force between lithium atoms is expected for this short distance. In contrast, for four lithium model, Li-Li distances are very close to the value of the bulk structure and the Li-Li interaction is expected to stabilize these lithium atoms. Therefore, we consider that Li-Li interaction is important for $N_{\mathrm{Li}} \geq 4$ for the (12,0) SWCNT. On the other hand, the Li-CNT distance is the longest for four lithium atoms. Hence, the stabilization of the four lithium model originates more significantly in the Li-Li interaction compared to other models. The decrease of the distance for six lithium atoms is due to the smallness of the cross section of the CNT. For six lithium atoms, lithium atoms does not occupy enough space, and hence they stay near the surface of the CNT. As a result, the six lithium structure is less stabilized than the four lithium

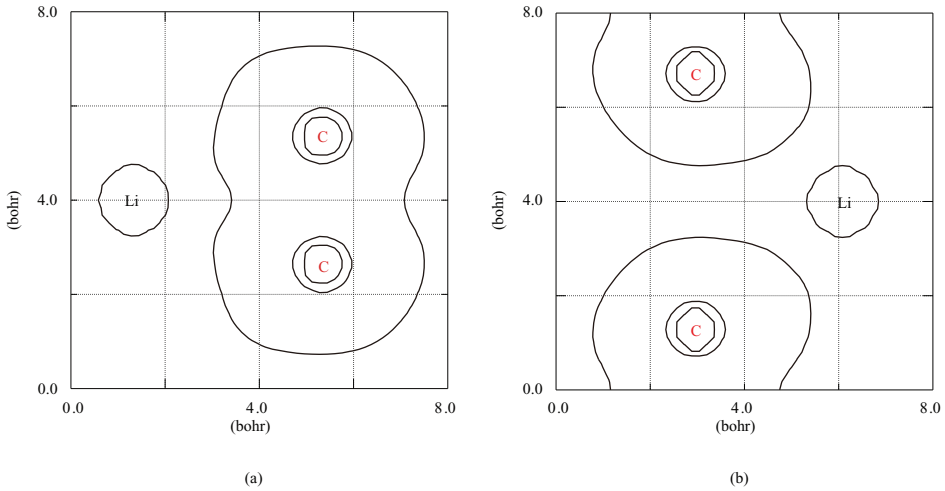

FIG. 4. The zero kinetic energy density surface. Panels (a) and (b) are the results of the lithium adsorption on the inside and outside of the CNT, respectively. Panel (b) (panel (d)) shows the plane including the Li, C(2), and C(3) atoms (Li, C(1), and C(4)), where a carbon atom specified in a parenthesis corresponds to that shown in Fig. 2.

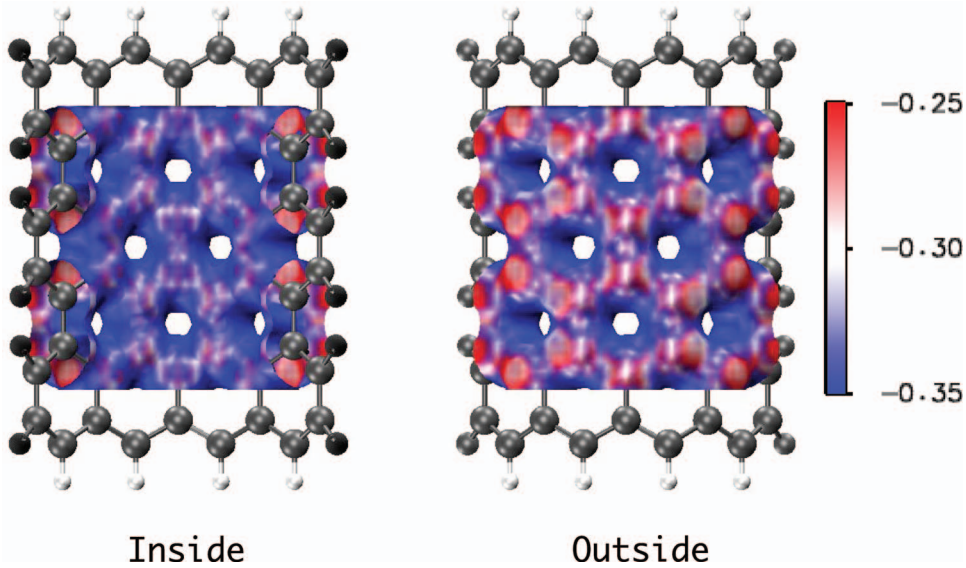

FIG. 5. Regional chemical potential density of our CNT model without the lithium atom on the zero kinetic energy surface.

one, due to the repulsion between lithium atoms arisen from this narrow space of the inside of the CNT.

Next, we discuss the difference of the stabilization in terms of the NBO charge of lithium atoms. In Fig. 8, the NBO charge is shown as the function of the number of lithium atoms. The solid line is the total charge, and the dashed line is the average for the charge per the number of lithium atoms. The average is small for $N_{\mathrm{Li}} \geq 3$, while the total charge is not small. The charge transfer is one of important factors for the stabilization of a system as attractive force between C-Li atoms and repulsive force between Li-Li atoms. For $N_{\mathrm{Li}} \leq 2$, the attractive force is dominantly important, since the average charge is the same for $N_{\mathrm{Li}} = 1$ and 2. On the other hand, the importance of the repulsive force is significant for $N_{\mathrm{Li}} \geq 3$, since the average value of charge is smaller than those for $N_{\mathrm{Li}} = 1$ and 2. Hence, the stabilization mechanism is not so simple and we study the charge transfer in detail below.

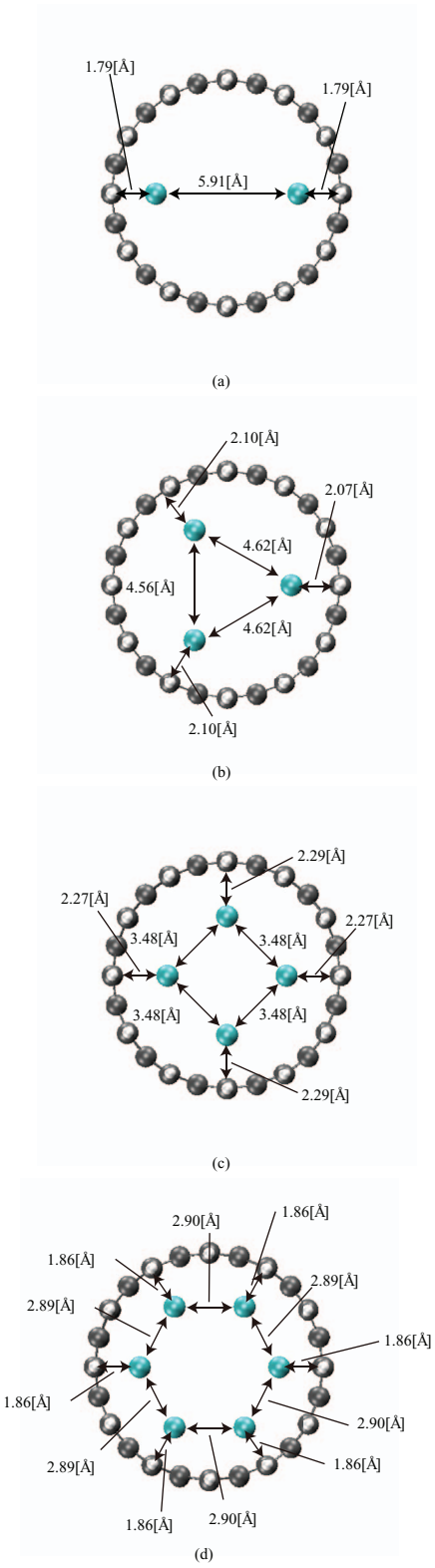

FIG. 6. The optimized structures of the models of (12,0) SWCNTs with lithium atoms. In panels (a)-(d), two, three, four, and six lithium atoms are attached on the inside of the CNT.

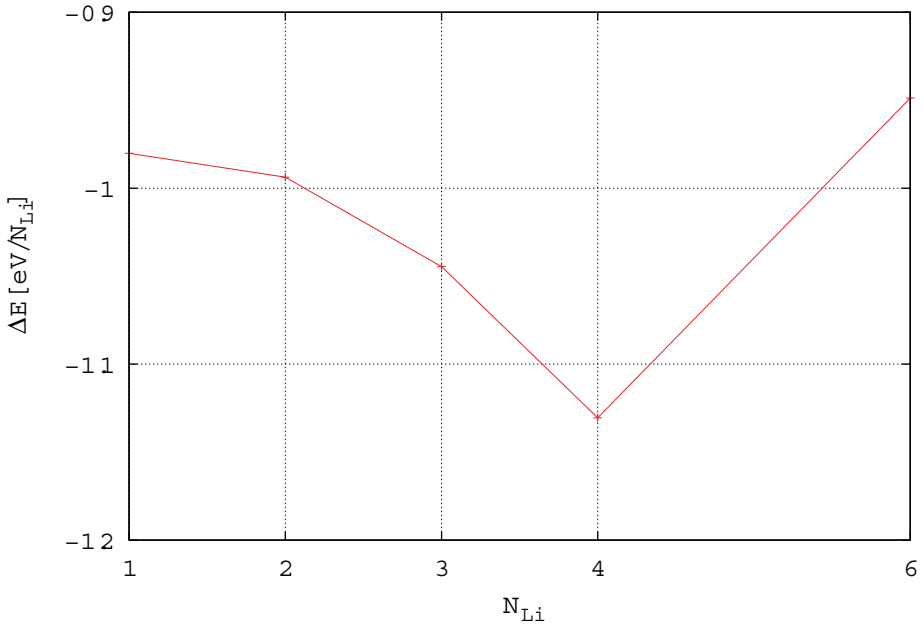

FIG. 7. Adsorption energy as the function of the number of lithium atoms.

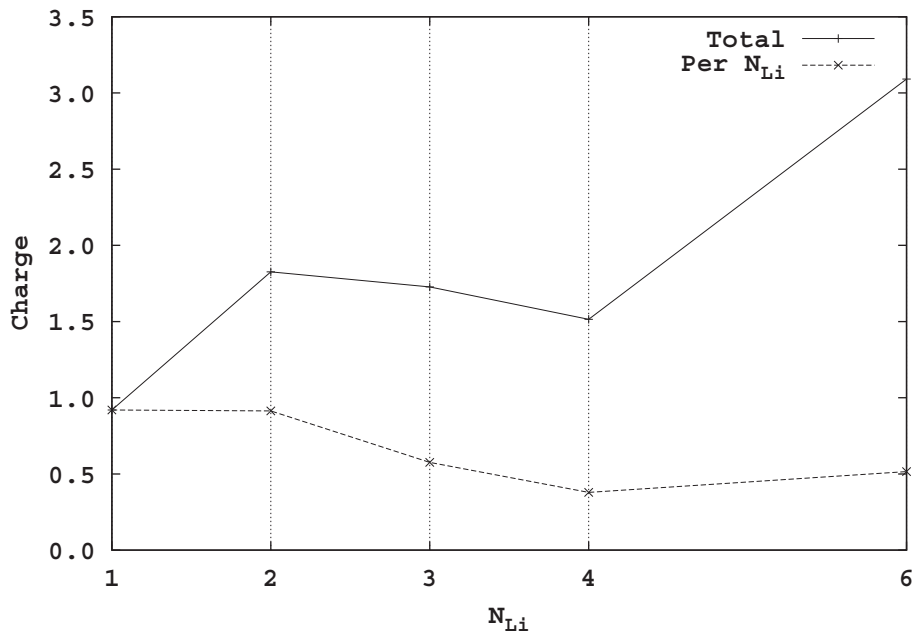

FIG. 8. NBO charge of lithium atoms as the function of the number of lithium atoms. The solid line is the total charge, and the dashed line is the average for the charge at the number of lithium atoms.

The distribution of the difference of electron density is shown in Fig. 9. Panels (a), (c), (e), and (g) show the plane perpendicular to the axis. Panels (b), (d), and (h) show the plane including the Li, C(2), and C(6) atoms, and panel (f) is for the Li, C(2), and C(5) atoms, where these carbon atoms are the nearest two C atoms. The circles in panels (a), (c), (e), and (g) mean the cross section of our CNT model. As seen in Fig. 9, electron density increase in the regions around carbons and between the nearest C atoms and the lithium atom as one lithium attachment. As seen in panels (a) and (b), the charge distribution difference for $N_{\mathrm{Li}} = 2$ is very similar to that for $N_{\mathrm{Li}} = 1$, and

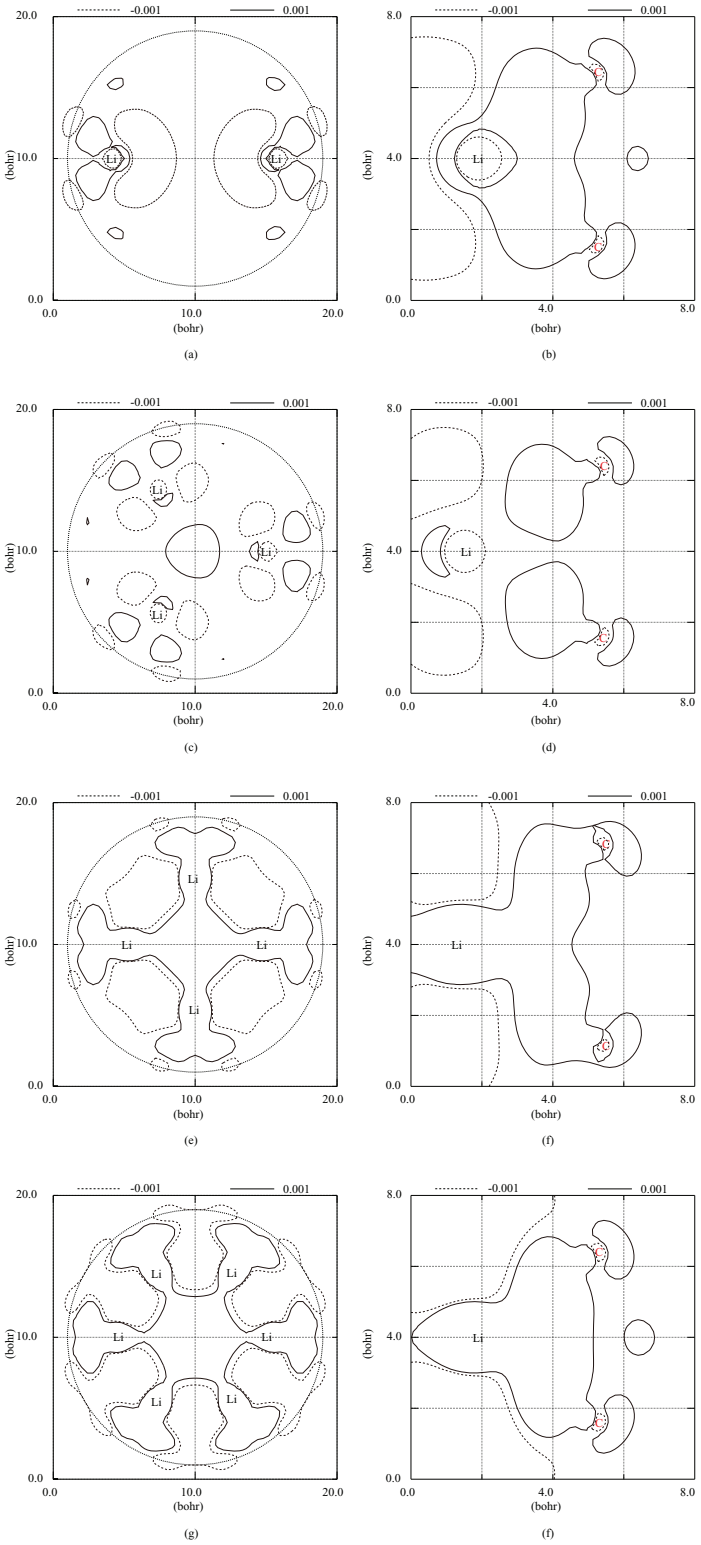

FIG. 9. Distribution of the difference of electron density. Panels (a), (c), (e), and (g) show the plane perpendicular to the axis. Panels (a), (c), (e), and (g) show the plane perpendicular to the axis. Panels (b), (d), and (h) show the plane including the Li, C(2), and C(6) atoms, and panel (f) is for the Li, C(2), and C(5) atoms, where these carbon atoms are the nearest two C atoms. The circle in panels (a), (c), (e), and (g) means the cross section of our CNT model.

hence the stabilization mechanism is also considered to be the same. For three, four, and six lithium atoms, the electron density around the center of the CNT increases. This is caused by repulsive force by negative charge stored in the CNT wall. It can also be said that this charge increase is induced by the repulsion between lithium atoms, since this feature is only seen for $N_{\mathrm{Li}} \geq 3$ due to the high density of lithium atoms. This charge increase arises from the narrow space in the CNT. As a result, the stabilization is not simply explained by the amount of charge transfer. Although the largest total charge transfer occured for $N_{\mathrm{Li}} = 6$, this large charge also induces large repulsive force between lithium atoms.

IV. CONCLUSIONS

In this study, we have investigated the adsorption of lithium atoms on the surface of the (12,0) zigzag CNT to clarify the interaction between lithium atoms and between a lithium atom and the CNT. For one lithium atom attachment on this CNT, it has been shown that the inside of this (12,0) zigzag CNT is more favorable than the outside. We have shown that after the lithium attachment, charge is transfered from the Li atom to the CNT and the bond between the Li atom and the CNT has ionic property. The amount of charge transfer is larger for the inside attachment than the outside. This feature is studied for the lithium atom adsorption on the (12,0) zigzag CNT in this work. The amount of charge transfer should be dependent on the curvature of the radius of a CNT, and hence it is important for us to investigate this feature for a CNT with different radius.

We have also shown that four lithium insertion for one layer of the carbon hexagon is the most stable. Our model have shown that the electron density around the center of the CNT increases significantly for $N_{\mathrm{Li}} \geq 3$. This increase originates in the repulsion between lithium atoms. For the six lithium atom structure, the distance between lithium atoms is shorter than that of the lithium bulk. Hence, the repulsive force between lithium atoms strongly destabilize the system. The structure of four lithium on one layer is much favorable compared to that of six.

ACKNOWLEDGMENTS

This work was partially supported by Grant-in-Aid from the Japan Society of the promotion of science (22550011). The computations were partially performed using Research Center for Computational Science, Okazaki, Japan.

[1] S. Iijima, Nature (London) **354** (1991) 56.
[2] C. T. White, T. N. Todorov, Nature **393** (1998) 240; J. Kong, E. Yenilmez, T. W. Tombler, W. Kim, H. Dai, R. B. Laughlin, L. Liu, C. S. Jayanthi, S. Y. Wu, Phys. Rev. Lett. **87** (2001) 106801; A. Javey, J. Guo, Q. Wang, M. Lundstrom, H. Dai, Nature (London) **424** (2003) 654.
[3] B. I. Yakobson, C. J. Brabeck, J. Bernholc, Phys. Rev. Lett. **76** (1996) 2511; J. P. Lu, Phys. Rev. Lett. **79** (1997) 1297.
[4] M. M. Treacy, T. W. Ebbesen, J. M. Gibson, Nature (London) **381** (1996) 678; E. W. Wong, P. E. Sheehan, C. M. Lieber, Science **277** (1997) 1971; A. Krishnan, E. Dujardin, T. W. Ebbesen, P. N. Yianilos, M. M. Treacy, Phys. Rev. B **58** (1998) 14013; S. Akita, H. Nishijima, T. Kishida, Y. Nakayama, Jpn. J. Appl. Phys. **39** (2000) 3724.
[5] N. Hamada, S. Sawada, A. Oshiyama, Phys. Rev. Lett. **68** (1991) 1579; R. Saito, M. Fujita, G. Dresselhaus, M. S. Dresselhaus, Phys. Rev. B **46** (1992) 1804; R. Saito, M. Fujita, G. Dresselhaus, M. S. Dresselhaus, Appl. Phys. Lett. **60** (1992) 2204;
[6] J. W. Ding, X. H. Yan, J. X. Cao, Phys. Rev. B **66** (2002) 073401; J. W. G. Wildöer, L. C. Venema, A. G. Rinzler, R. E. Smalley, C. Dekker, Nature (London) **391** (1998) 59; T. W. Odom, J.-L. Huang, P. Kim, C. M. Lieber, J. Phys. Chem. **104** (2000) 2794; S. Reich, C. Thomsen, P. Ordejón, Phys. Rev. B **65** (2002) 155411.
[7] J. Zhao, A. Buldum, J. Han, J. P. Lu, Phys. Rev. Lett. **85** (2000) 1706.
[8] For a review, M. Inagaki, "New Carbons Control of Structure and Functions", Chap. 6, Elsevier, Amsterdam (2000).
[9] B. Gao, A. Kleinhammes, X. P. Tang, C. Bower, L. Fleming, Y. Wu, O. Zhou, Chem. Phys. Lett. **307** (1999) 153; G. Maurin, Ch. Bousquet, F. Henn, P. Bernier, R. Almairac, B. Simon, Chem. Phys. Lett. **312** (1999) 14.
[10] Z. Yang, H. Wu, Solid State Ionics **143** (2001) 173; S. Komiyama, M. Miyawasi, F. Okino, H. Kataura, H. Touhara, TANSO **216** (2005) 25 (in Japanese).
[11] S. Kawasaki, Y. Iwai, I. Watanabe, Mater. Res. Bull. **44** (2009) 415.
[12] S. Sano, M. Kusunoki, A. Tachibana, *The 50th Battery Symposium in Japan*, Abstract No. 3A21 (2009).
[13] A. Tachibana, Theor. Chem. Acc. **102** (1999) 188; P. Szarek, Y. Sueda, and A. Tachibana, J. Chem. Phys. **129** (2008) 094102.

[14] S. Pawel, A. Tachibana: J. Mol. Modeling **13** (2007) 651; P. Szarek, K. Urakami, C. Zhou, H. Cheng, A. Tachibana, J. Chem. Phys. **130** (2009) 084111.
[15] C. Lee, W. Yann, and R. G. Parr, Phys. Rev. B **37** (1988) 785.
[16] A. D. Becke, J. Chem. Phys, **98** (1993) 5648.
[17] M. J. Frisch *et al.*, Gaussian 03, Revision B.05, Gaussian, Inc., Pittsburgh PA (2003).
[18] W. J. Hehre, R. Ditchfield, J. A. Pople, J. Chem. Phys. **56** (1972) 2257; J. D. Dill, J. A. Pople J. Chem. Phys. **62** (1975) 2921.
[19] P. C. Hariharan, J. A. Pople, Theo. Chim. Acta **28** (1973) 213.
[20] J. S. Binkley, J. A. Pople, W. J. Hehre, J. Am. Chem. Soc. **102** (1980) 939.
[21] T. Pankewitz, W. Klopper, J. Phys. Chem. C **111** (2007) 18917.
[22] A. Tachibana, R. G. Parr, Int. J. Quantum Chem. **41** (1992) 527; A. Tachibana, Int. J. Quantum Chem. **32** (1987) 181; Int. J. Quantum Chem. **57** (1996) 423; Int. J. Quantum Chem. **100** (2004) 981; A. Tachibana, K. Nakamura, K. Sakata, T. Morisaki, Int. J. Quantum Chem. **74** (1999) 669; A. Tachibana, J. Chem. Phys. **115** (2001) 3497; A. Tachibana, *Stress Induced Phenomena in Metallization*, ed. S. P. Baker (American Institute of Physics, New York, 2002), pp. 201-211; A. Tachibana, *Reviews in modern quantum chemistry:A celebration of the contribution of Robert Parr* ed. K. D. Sen (World scientific, Singapore, 2002) Vol. **2**, pp. 1327-1366; A. Tachibana, *Fundamental Perspectives in Quantum Chemistry: A Tribute to the Memory of Per-Olov Löwdin*, ed. E. J. Brrmändas and E. S. Kryacho (Kluwer Academic, Dordrecht, 2003) vol. **II**, p. 211.
[23] A. Tachibana, J. Mol. Modeling **11** (2005) 301; A. Tachibana, J. Mol. Struct.: (THEOCHEM) **943** (2010) 138.
[24] M. Senami, K. Ichikawa, K. Doi, P. Szarek, K. Nakamura, A. Tachibana, *Molecular Regional DFT program package*, ver. 3 (Tachibana Lab., Kyoto University, Kyoto, 2008).
[25] W. Andreoni, A. Curioni, Appl. Phys. A **66** (1998) 299; T. Aree, T. Kerdcharoen, S. Hannongbua, Chem. Phys. Lett. **285** (1998) 221.
[26] P. Dubot, P. Cenedese, Phys. Rev. B **63** (2001) 241402(R).
[27] V. Meunier, J. Kephart, C. Roland, J. Bernholc, Phys. Rev. Lett. **88** (2002) 075506.
[28] A. A. Kuzubov, P. V. Avramov, S. G. Ovchinnikov, S. A. Varganov, F. N. Tomilin, Phys. Sol. State **43** (2001) 1721.